

## Synthesis and Properties of New Paramagnetic Hybrid Bayerite from Al(0)/Naphthalene Dianhydride Reaction

Eduardo Rezende Triboni<sup>a,\*</sup>, Mauro Francisco Pinheiro da Silva<sup>a</sup>, Alan Teruel Finco<sup>a</sup>,

Magali Aparecida Rodrigues<sup>a</sup>, Grégoire Jean-François Demets<sup>c</sup>, Fabio Henrique Dyszy<sup>a</sup>,

Paulo Celso Isolani<sup>b</sup>, Pedro Berci Filho<sup>b</sup>, Mario José Polit<sup>a</sup>

<sup>a</sup>Instituto de Química, Universidade de São Paulo – USP,

Av. Prof. Lineu Prestes 748, CEP 05508-900, São Paulo, SP, Brazil

<sup>b</sup>Instituto de Química de São Carlos, Universidade de São Paulo – USP,

Av. Trabalhador São Carlense 400, CEP 13566-590, São Carlos, SP, Brazil

<sup>c</sup>Departamento de Química, Faculdade de Filosofia Ciências e Letras de Ribeirão Preto,

Universidade de São Paulo – USP, Av. Bandeirantes 3900,

CEP 14040-901, Ribeirão Preto, SP, Brazil

Received: July 26, 2010; Revised: October 30, 2010

The reaction of Naphthalene 1,4,5,8-dianhydride (NTCDA) with elemental aluminum(0) powder is studied in an aqueous alcoholic KOH mixture to search for the NTCDA anion and dianion electron-adducts. After analyzing various reaction conditions it was found that the reaction yielded a greenish precipitate in 3:1 (v:v) ethanol:water mixture. This powder is composed mainly of aluminum trihydroxide crystallites of bayerite [ $\alpha$ -Al(OH)<sub>3(s)</sub>] and the organic content is approximately 6%. This hybrid material proved to be paramagnetic even after exposure to air for one year and at temperatures up to 200 °C. Typical carbonylic bound to metal IR bands and reflectance UV-VIS spectra demonstrate the entrapment of NTCDA radical anion into the aluminum trihydroxide, hence rendering its green color and a paramagnetic behavior. Thus, besides the understanding of an aluminum reaction in suspension, the entrapment of an organic material (NTCDA) that stays stable as the corresponding radical can provide an interesting option for the synthesis of aluminum trihydroxide composites.

**Keywords:** aluminum, naphthalene 1,4,5,8-dianhydride, bayerite [ $\alpha$ -Al(OH)<sub>3(s)</sub>], paramagnetic hybrid material

### 1. Introduction

Naphthalene 1,4,5,8-tetracarboxylic dianhydride (NTCDA) is the reagent of choice for obtaining diimide derivative compounds<sup>1-3</sup>. It is also used for the design and preparation of molecule-based materials (MBM's)<sup>4</sup> such as molecular-electronic components, electro luminescent devices and photoconductors materials<sup>5-8</sup>. Relevant properties for these applications are related to the  $\pi$ -conjugated bond system within a planar molecular structure and also to the high electron-affinity of NTCDA, as well as its derivatives. Spectroscopic characterizations by magnetic circular dichroism (MCD)<sup>9</sup>, UV-VIS spectroscopy and luminescence<sup>10</sup> have established the nature of the electronic transition and the character of the ground and excited electronic states. In addition, kinetic and computational studies dealing with NTCDA aqueous hydrolysis have demonstrated the stability of the various forms, such as the mono and diacid anhydride, as a function of pH<sup>11</sup>. An important feature of NTCDA is the stability of the NTCDA<sup>-</sup> radical anion and NTCDA<sup>2-</sup> dianion.

The electron-adduct species have been characterized by electrochemical<sup>12</sup> and spectroscopic methods such as electron spin resonance ESR<sup>13</sup> and UV-VIS spectrophotometry<sup>12</sup>. Both reduced species display electronic transitions in the visible region that markedly differ from that of the parent compound. Moreover, crystalline salts based on anion radical salts of naphthalene tetracarboxylic acid derivatives have been prepared for application

as electron conducting compounds<sup>14</sup>. Another feature of NTCDA derivatives is their thermal stability that allows thermal treatments up to ~450 °C without chemical or physical decomposition<sup>15</sup>.

Bayerite is one of the four forms of naturally occurring aluminum trihydroxide crystallites, the others are polymorphic modifications known as gibbsite, nordstrandite, and doyleite<sup>16</sup>. In the chemical industry, gibbsite and bayerite are used as the main components in antacid drugs, alumina-supported catalysts, as support in the catalytic cracking process, and as adsorbents in chromatography and manufacturing of several materials<sup>16-20</sup>. Despite its industrial applications, it is important to understand the factors that influence the growth as well as the crystal morphology of these aluminum trihydroxides<sup>21</sup>. The precipitation of aluminum trihydroxides is considered a crucial step in the Bayer process therefore several syntheses start from highly concentrated sodium or potassium aluminate solutions<sup>22-24</sup>. Recently, bayerite has received attention in the preparation of a prominent class of materials, namely layer double hydroxides, LDH<sup>25-27</sup>. Bayerite has been synthesized by ageing the alumina gels in water, acidification of aluminate solutions by use of HClO<sub>4</sub>, HNO<sub>3</sub> and or CO<sub>2</sub>, and from aluminum powder in alkaline media<sup>28-31</sup>. It is not wrong to affirm that the synthesis methodology plays an important role in the crystallite properties and hence in the final material properties.

\*e-mail: triboni@iq.usp.br

Elemental aluminum Al(0) is considered a “pool” of electrons for chemical reactions due to its high oxidation potential ( $\text{Al}/\text{Al}^{3+} = 1.67 \text{ V vs. SCE}$ ) and the three electrons available<sup>32</sup>. It is largely used in bimetallic systems involving metal/metal-salts that act as reducing agents<sup>33</sup>, also Al(0) powdered suspensions are used in the reduction of nitro and of carbonylic functionalities carried out with basic or acidic conditions in protic solvents<sup>34,35</sup>. Since organometallic reductions commonly start through a single electron transfer (SET process) to the organic partner<sup>36,37</sup>, the use of this metal with organic species that have the ability to form stable electron-adduct products could be a good strategy to obtain paramagnetic hybrid organic-inorganic composites based on aluminum trihydroxide matrix.

In this work, besides the aluminum NTCDA-reduction reaction features in solvents and binary mixtures, a new paramagnetic hybrid inorganic-organic material based on bayerite matrix [ $\alpha\text{-Al}(\text{OH})_3$ ] and NTCDA electron-adducts is presented (disperse phase), prepared from direct precipitation of the alkaline solution containing aluminates and NTCDA-reduced species in a specific water-ethanol mixture. The ideal condition was achieved using 75% ethanol in water (v:v). Thus, a greenish powder was formed that after characterization showed to be a paramagnetic aluminum hydroxide. By UV-VIS reflectance spectroscopy, FTIR, and ESR spectra, the entrapment of NTCDA radical-anion species was evidenced. Powder X-ray diffraction evidenced aluminum hydroxide crystallites of bayerite. Furthermore, this material showed to be visually stable (no color fading) even after long air exposure. Following these observations, the experimental details of aluminum NTCDA reaction and the properties of the bayerite-NTCDA material are reported, as well its partial characterization. In the present study the reaction of Al(0) and NTCDA in water/alcohol mixtures allowed the preparation of a controlled and defined crystalline aluminum hydroxide, and as well the preparation of an organic-inorganic hybrid material with air-stable paramagnetic properties.

## 2. Experimental

**Materials:** Naphthalene 1,4,5,8-tetracarboxylic dianhydride (NTCDA) and naphthalene 1,4,5,8-tetracarboxylic acid (NTCac) were purchased from Aldrich and used without further purification. Aluminum powder (Reagent) and ethanol (Mallinkrodt) were used as received. Water was doubly distilled and further purified via a Millipore Milli-Q system; others solvents and reagents were of the best available purity.

**Survey of NTCDA-Aluminum/KOH reaction conditions:** Several reaction conditions tested as base and Al(0) proportions, aprotic solvents as THF, DMF, dioxane, acetonitrile and as well pure water or ethanol did not result in the adduct formation. Water-alcohol binary mixtures showed to be the appropriate solvent system and in ethanol or methanol aqueous mixtures the NTCDA reduction occurred promptly with the hydrolysis as a side reaction. The subsequent assays were conducted in water-ethanol mixtures. It should be noted that in acidic media there was no trace of reduction even using stronger mineral acid conditions and as previously seen, no hydrolysis occurred<sup>11</sup>.

**Al-NTCDA/KOH reactions in suspension:** an excess of aluminum powder (~8 mmol, 200 mg) was added to NTCDA (1 mmol, 268 mg) in 20 mL water:ethanol 3:1 v:v (15:5 mL) containing KOH (560 mg, 10 mmol or 300 mg, 5.3 mmol) in an Erlenmeyer flask under magnetic stirring at room temperature. The reactions were highly exothermic and gas evolving ( $\text{H}_2$ ). These conditions were selected to investigate by standard UV-Vis spectroscopy, which were the NTCDA electron-adduct generated species. Accordingly, the amount of KOH varied from 5.3 to 10 mmol.L<sup>-1</sup> in order to enable the increase of the redox potential of the Al(0).

**NTCDA-bayerite powder preparation:** aluminum powder, Al(0), (~8 mmol, 200 mg) was set to react with NTCDA (1 mmol, 268 mg) and KOH (10 mmol, 560 mg) in 20 mL ethanol:water 3:1 v:v (15:5 mL) (notice the higher amount ethanol compared to the reaction in suspension) in an Erlenmeyer flask under magnetic stirring at room temperature. The reactions were highly exothermic and gas evolving ( $\text{H}_2$ ). After twenty minutes a green solid precipitated. The solid was filtered, washed with distilled water and ethanol and dried in an oven at 150 °C, yielding 600 mg of powder. This solid was characterized by ESR, UV-VIS diffuse reflectance spectrophotometry, FTIR, and electrical conductivity.

**Analytical Methods:** the UV-VIS absorption spectra of the mixtures were recorded using a Shimadzu UV-2400-PC spectrophotometer. Spectral data were obtained using quartz cuvettes with 1 cm optical path length. The UV-VIS spectra of the powders were recorded by diffuse reflectance with a USB 200 photometer (Ocean Optics) using MgO as reflectance standard. FTIR (Bomen model MB 100) measurements were performed on KBr pellets in the range 4000 to 500 cm<sup>-1</sup>. Electronic Spin Resonance (ESR) spectra were obtained in an ESP-300 Bruker spectrometer. Energy Dispersive X-ray (EDX) analysis were made in a Thermo Electron Co. apparatus. Electrical conductivity measurements were carried out at room temperature using a homemade two-point probe method<sup>38</sup>. Conductivities ( $\sigma$ ) were obtained according to the formula:  $\sigma = (I/S) \cdot (V/I)$ , where V is the bipolar tension, I is the continuous electrical current across the sample, l is the bipolar distance, and S is the sample cross-sectional area<sup>38</sup>. XRD diffraction patterns were obtained on an X-ray Diffractometer Rigaku Miniflex (30 kV/15 mA), using a Cu tube, K $\alpha$ ,  $\lambda = 1.54 \text{ \AA}$  with Ni filter.

## 3. Results and Discussion

### 3.1. Al-NTCDA reduction reactions in suspension in mild and high KOH conditions: electron adducts assignments

Figures 1 and 2 show the electronic spectra of the species obtained when NTCDA was reacted with KOH and Al in water:ethanol (3:1, v:v) suspension in mild (300 mg KOH) and more alkaline (560 mg KOH) conditions, respectively. Using the mild condition, the suspension initially turned into a red brown color with the spectrum exhibiting a broad band at around 464 nm that vanished after 2 hours (Figure 1). These characteristics are similar to that observed for the corresponding diimide radical anion formed through photochemical reactions from its triplet state<sup>39,40</sup> and to the NTCDA<sup>-</sup> radical anion spectra observed upon electrochemical reduction<sup>12</sup>. After the disappearance of the radical species only the transitions at 310 and 232 nm corresponding to the NTCDA hydrolysis product spectrum are observed, in other words the naphthalene 1,4,5,8-tetra acid, NTCac, (Figure 2 inset).

In strong alkaline media the suspension instantly turns bright green (Figure 2). This color is due to an electronic transition having absorption maximum at  $\lambda = 396 \text{ nm}$  and less intense bands appearing at 670, 614, and 564 nm respectively. These features are in agreement with those known for the doubly charged NTCDA<sup>2-</sup> produced via electrochemical reduction of NTCDA<sup>12</sup>. However, the naphthalene dianhydride dianion spectrum obtained in this metal ion suspension presents a large bathochromic shift when compared to diimide dianion spectra in solution which exhibit peaks at 600, 550 and 510 nm<sup>40</sup>. Despite the bathochromic shift the spectrum features of the diimide and dianhydride dianions are similar and show the same vibronic spacing of ~1.4 cm<sup>-1</sup>. After two hours, as observed in weak alkaline media, the color fades and the spectrum becomes similar to that of NTCac (Figure 2 inset).

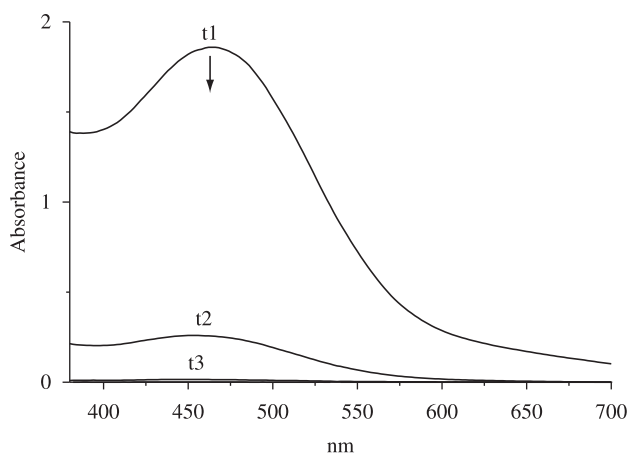


**Figure 1.** Reaction of NTCDA with Al and  $\text{OH}^- = 300$  mg, in 20 mL  $\text{H}_2\text{O-EtOH}$  (15:5 mL), t1, t2 and t3 correspond 45 minutes time interval between each UV-VIS spectrum.

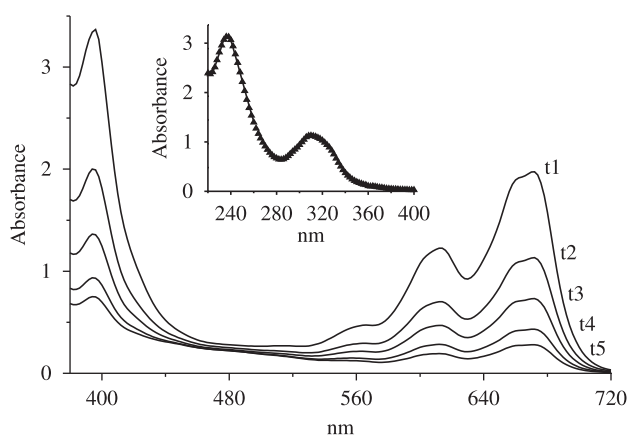


**Figure 2.** Reaction of NTCDA with Al and  $\text{OH}^- = 500$  mg, in 20 mL  $\text{H}_2\text{O-EtOH}$  (15:5 mL). UV-VIS spectrum from t1 to t5 timespan was 2 hours with 25 minutes interval. Insert: naphthalene 1,4,5,8-tetracarboxylic acid UV-VIS spectrum with maximum absorption peaks at  $\lambda_{\text{abs}}^{\text{max}} = 230$  and 310 nm.

Higher concentrations of base give rise to the NTCDA dianion, whereas in lower base concentrations the monoanion is favored, evidencing that the formation of NTCDA electron adduct species depends on the base concentration. This can be understood based on the potential aluminum oxidation with pH variation. This potential increases linearly with the base concentration in aqueous media<sup>41,42</sup>. In addition, the available literature standard potential ( $E^\circ$ ) values for  $\text{NTCDA}^{1-}$  and  $\text{NTCDA}^{2-}$  formation from NTCDA are  $E^\circ = -0.28$  V and  $E^\circ = -0.69$  V (SCE), respectively, in DMF<sup>12</sup>. Therefore, the base concentration increase should favor two-electron reduction of NTCDA by aluminum. This pH-dependent reduction potential explains the lack of reactivity in acidic media<sup>41,42</sup>.

So, in the reaction system Al-NTCDA/ $\text{OH}^-$  carried out in water:ethanol (3:1, v:v) besides the electron transfer reaction, dianhydride hydrolysis occurs to a high degree. In both assays the spectra of the final product are similar to that of NTCac, as expected. In the experimental conditions the reduced NTCDA species,  $\text{NTCDA}^{1-}$  and  $\text{NTCDA}^{2-}$ , are stable in solution for approximately 2 hours. These species could be maintained longer in an inert atmosphere.

### 3.2. Water-ethanol mixture, aluminum and base effects on Al-NTCDA reaction

The use of two different proportions of  $\text{H}_2\text{O:EtOH}$  (3:1 or 1:3, v:v) and amounts of potassium hydroxide showed a significant influence on the Al-NTCDA reaction. As described in the previous section with the use of water as the predominant solvent ( $\text{H}_2\text{O:EtOH}$ , 3:1, v:v),  $\text{NTCDA}^{1-}$  radical anion and  $\text{NTCDA}^{2-}$  dianion were obtained for proportions of NTCDA/Al(0)/KOH (1/8/10 mole ratios) and NTCDA/Al(0)/KOH (1/8/5 mole ratios) respectively. A significant formation of hydrolysis products was also verified in these aqueous media.

On the other hand, when the reaction was carried out with the alcohol as the main solvent ( $\text{H}_2\text{O:EtOH}$ , 1:3 v:v) and with NTCDA/Al(0)/KOH (1/8/10 mole ratios) a new situation was obtained in which a green precipitate was immediately formed and upon characterization it was identified as a composite constituted of an aluminum trihydroxide bayerite matrix bearing NTCDA electron adducts. This specific  $\text{H}_2\text{O:EtOH}$  (1:3, v:v) solvent condition in which the aluminum NTCDA reduction was conducted led to the predominant aluminum trihydroxide bayerite high yield precipitation and in a short reaction time. It can therefore be considered as a selective medium for bayerite and for bayerite based composites formation.

Recently, Antunes and co-workers<sup>21</sup> conducted a systematic study concerning the effect of water-alcohols mixtures on the crystallization of non-crystalline  $\text{Al}(\text{OH})_3$ . It was found that the ethanol in the aqueous binary mixture had different effects according to its percentage: 20% produced bayerite + nordstrandite + fibrillar pseudoboehmite, 50% yielded gibbsite + bayerite + pseudoboehmite, and 94% yielded only fibrillar pseudoboehmite. The alteration in the formation of somatoids of bayerite from non-crystalline  $\text{Al}(\text{OH})_3$  in other aluminum hydroxide types with other alcohols added was also reported. In addition, the use of methanol in the Bayer process improved the precipitation of gibbsite from the supersaturated sodium aluminate solution<sup>43</sup>. However, alcohols exert an important driving force over seeded precipitation of these aluminum hydroxides in aluminate solutions.

The effects of the nature of the base and metal amount on NTCDA reduction behavior were evaluated. The reactions were carried out in  $\text{H}_2\text{O:EtOH}$  (3:1, v:v) to avoid precipitation of the bayerite. Sodium and potassium hydroxides were more effective for the reduction and for aluminum consumption than sodium, potassium or cesium carbonates and also ammonium and lithium hydroxides. The increase of aluminum molar excess from five-fold to eight-fold with respect to the anhydride did not change the reaction profile.

It is known that in aqueous solution the aluminum consumption is highly dependent on its own concentration, pH, nature and type of counterion of the base, and stability of the aluminate species in the reaction media<sup>41,42,44,45</sup>. Besides the solvent effects, to obtain NTCDA electron adducts, the reaction efficiency was also found to depend on the nature of cations and the amount of base added. However, reaction efficiency appears to be related to the characteristics of aluminum leaching process in aqueous alkaline condition. In this process the hard oxide shell recovering the metal is first dissolved<sup>46,47</sup> with the metal becoming free and active to be oxidized<sup>41,42,48</sup>, hence generating a complex mixture of aluminum complexes in solution. For instance, studies on aluminum chemical speciation reveal the presence of monomeric and oligomeric aluminates ranging from 6- to 5- and 4-coordination numbers, all of them in a very narrow pH range<sup>49-51</sup>. Apart from this, aluminum solution chemistry is an unresolved theme with several open questions<sup>50,51</sup>.

Taking into account the aforementioned, four main points can be considered for the Al-NTCDA/ $\text{OH}^-$  reduction system in water-ethanol mixtures: i) in strong aqueous alkaline media besides the NTCDA high hydrolysis rate constant and its lower solubility, aluminate species are soluble and therefore no bayerite is formed in short

reaction times; ii) in pure alcoholic media, as in other organic solvents, no aluminum corrosion and consequently no NTCDA reduction occurs; iii) in mixed water-ethanol media these two constraints are relaxed and so, solubilization of NTCDA and its redox reaction are highly favorable; iv) at the same time, in the specific H<sub>2</sub>O-EtOH 1:3 mixture ratio, electron adduct NTCDA species are formed and the aluminate solution is destabilized, leading to the precipitation of bayerite. This solvent tendency is summarized in Figure 3.

Following, using any of the proportions already mentioned for the adduct formation of other aromatic di-anhydrides such as 3,4,9,10-perylene and 1,2,4,5-benzene tetracarboxylic and also mono anhydrides such as 1,8- and 2,3-naphthalene and phthalic, the Al(O)/OH<sup>-</sup>/H<sub>2</sub>O-EtOH system did not work. A result associated with redox potential of the compounds above. The reaction was also tested with 1,4,5,8-naphthalene tetracarboxylic acid (NTCac) and again no reaction was detected.

### 3.3. NTCDA-bayerite powder characterization

The XRD pattern of the green solid presented in Figure 4 shows the crystalline character of this solid. The solid obtained in the absence of NTCDA showed the same XRD pattern, indicating that both powders have similar crystallographic structures. The solids were identified as bayerite [ $\alpha$ -Al(OH)<sub>3</sub>], ICSD 200413, with space group P2<sub>1</sub>/n<sup>17,52</sup>. The bayerite has a layered structure composed by sheets of aluminum coordinated by six OH<sup>-</sup> (a double layer of hydroxides), forming an Al(OH)<sub>6</sub> with octahedral aluminum structure, where

two hydroxides are shared by neighboring aluminum centers. The cohesion between two consecutive sheets is ensured by inter-layer hydrogen bonds<sup>16,17</sup>.

Figure 5 shows the ESR spectrum of the NTCDA-bayerite. A line of symmetric shape without hyperfine structure is observed. The g value determined is 2.006, typical of organic radical anions and with relatively free paramagnetic species<sup>53,54</sup>. This result indicates that there is at least one paramagnetic species entrapped in the bayerite, which can be attributed to the NTCDA radical anion, NTCDA<sup>•-</sup>. The paramagnetic signal remains unchanged for a long time, even under air exposition. For instance, a preparation left on the bench for more than a year still presented the green color due to the radical. Another preparation was left in an oven at 200 °C for more than one month and even in these conditions the radical was stable.

The electronic conductivities of both the NTCDA-bayerite and “pure” bayerite powders were measured to be approximately 10<sup>-6</sup> S.cm<sup>-1</sup> showing that the paramagnetic species does not influence the conduction of bayerite and thus the conduction must occur through ion motion<sup>55</sup>.

The electronic reflectance UV-VIS spectra of NTCDA and NTCDA-bayerite composite are shown in Figure 6. The spectrum of NTCDA presents a broad band ranging from 220 to 430 nm and two peaks at 375 and 402 nm. However, the NTCDA-bayerite spectrum shows a remarkable difference, with the presence of well-defined bands peaking at 245, 309, 384, and 432 nm. Also, a new broad band appears covering practically all the visible-region from 490 to 840 nm.

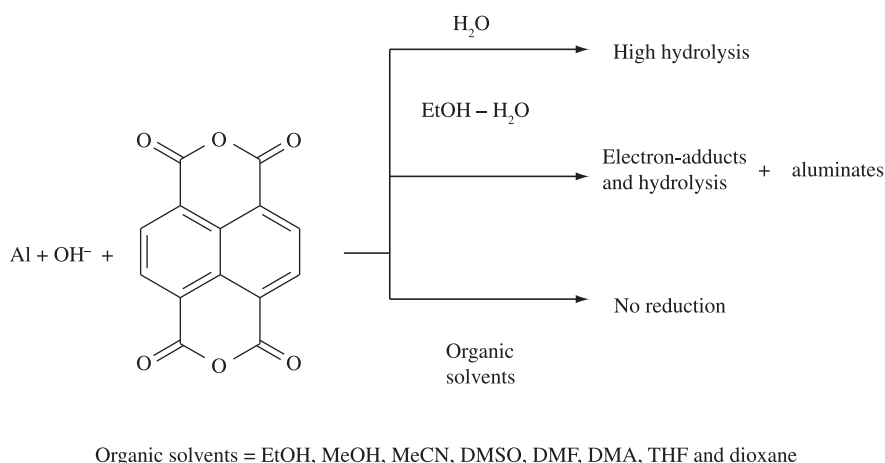


**Figure 3.** Role of the solvents on NTCDA-Al(O)/OH<sup>-</sup> reaction.

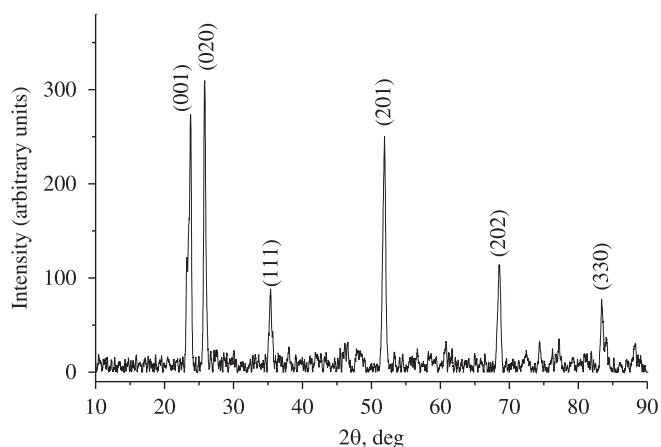


**Figure 4.** X-ray diffraction pattern of NTCDA-bayerite powder.

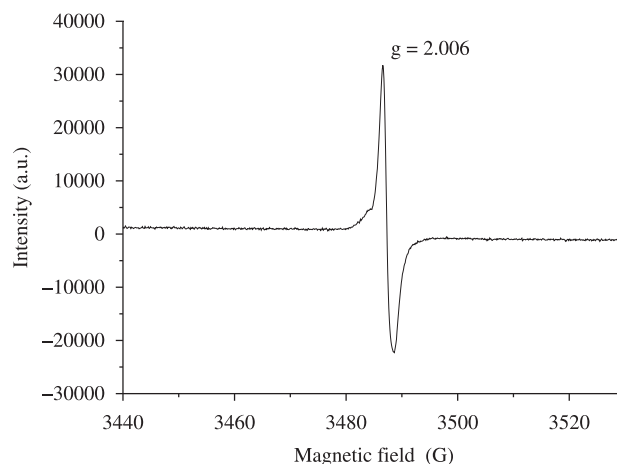


**Figure 5.** ESR spectrum of NTCDA-bayerite powder.



In a related work Tachikawa and co-workers<sup>53</sup>, studying NTCDA-aluminum films formed by vacuum deposition, obtained a UV-VIS spectrum whose band profile is similar to that shown in Figure 6 for NTCDA-bayerite. The ESR spectrum showed a signal of an unbound electron resembling the one reported here for the paramagnetic radical species. As an interpretation of the UV-VIS and ESR spectra, the authors suggested a charge transfer from the aluminum surface to the NTCDA carbonyl groups. In addition, the broad and red-shifted UV-VIS absorption band suggests an electronic cross talk between neighboring molecules as is typical of excited- and ground-state and anion radical  $\pi$ -aggregates of naphthalene derivatives<sup>14,15,56,57</sup>.

The infrared absorption spectrum of NTCDA presents a strong peak at  $\sim 1780\text{ cm}^{-1}$  due to the dianhydride carbonylic group<sup>53</sup>. Tachikawa reported that when NTCDA was deposited onto the aluminum surface a less intense one at  $1715\text{ cm}^{-1}$  substituted this transition. The IR data of NTCDA-bayerite presented in Figure 7 shows the presence of a carboxylate-bayerite complex material as evidenced by the large band with a strong peak at  $1591\text{ cm}^{-1}$ <sup>[58]</sup> and shoulders at  $1697, 1541, 1504\text{ cm}^{-1}$  that can be attributed to carbonyl stretching of the acid functionality, while the peak at  $1720\text{ cm}^{-1}$  is a strong indicative of the presence of one-electron reduced naphthalene dianhydride as reported by Tachikawa. Therefore, the bayerite obtained in this work seems to have the naphthalene tetracarboxylic acid, NTCac, and the non-hydrolyzed NTCDA reduced form. Figure 7 also shows hydroxyl stretching of bayerite at  $3659, 3553,$  and  $3459\text{ cm}^{-1}$ <sup>[17]</sup>.

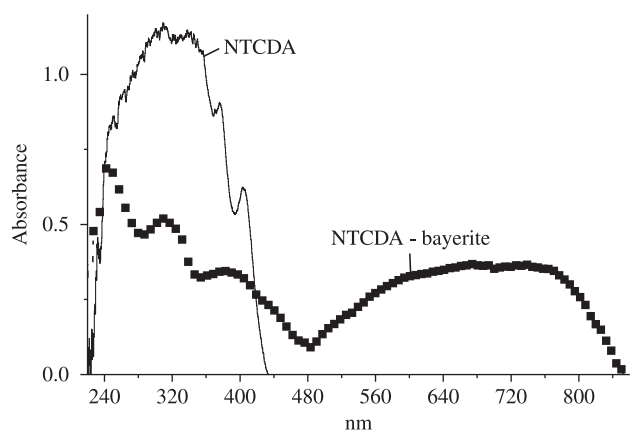


**Figure 6.** UV-VIS spectra of the pure NTCDA powder and NTCDA-bayerite powder recorded by diffuse reflectance.

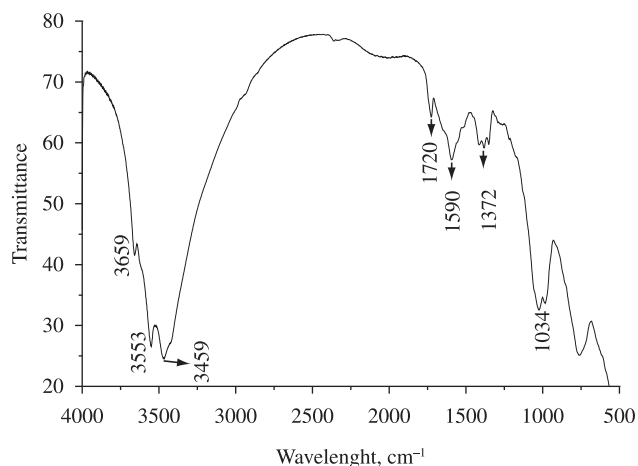


**Figure 7.** FTIR of the NTCDA-bayerite.

On the other hand, in the present work, the formation of the NTCDA radical anion was achieved in experimental conditions quite different from that carried out by Tachikawa (as well as the material obtained). Thus, it is tempting to consider another kind of mechanism in which the NTCDA radical anion (NTCDA<sup>1-</sup>) is previously formed in solution by aluminum reduction and subsequently incorporated into the layered double hydroxide sheets of the bayerite structure through hydrogen bonds between the hydroxides and the anhydride's carbonyls. Taking into account that the elemental analysis of the material found 6% of organic content and that NTCDA radicals in solution are stable up to two hours under atmospheric conditions, against at least one year into the bayerite matrix, it is plausible to consider that within the hybrid material structure the organic radicals are protected from oxygen, probably placed between consecutive sheets (Figure 8).

The formation of bayerite from aluminum in alkaline solution is considered to be through the pre-aggregation of monomeric  $\text{Al}(\text{OH})_4^-$  with increasing  $\text{Al}^{3+}$  and  $\text{OH}^-$  concentrations. Calculations demonstrated that polymeric aluminum hydroxo complexes, like  $\text{Al}_6(\text{OH})_{22}^{4-}$ , are formed initially, followed by the deposition of bayerite [ $\alpha\text{-Al}(\text{OH})_3$ ] crystallites<sup>24</sup>. In addition, kinetic studies of bayerite microstructure formation from aluminum powder found porous aluminum hydroxides that are formed through the previous dissolution of initial aluminum particles<sup>59</sup>. Moreover, Rat'ko and co-workers<sup>60</sup> reported that the interphase  $\text{Al}/\text{Al}(\text{OH})_3$  composite is composed of porous agglomerates of bayerite crystallites.

These data are indicative that in NTCDA- $\text{Al}/\text{OH}^-$  reaction some molecules of NTCDA, before being hydrolyzed, can interact with the aluminum surface, so the NTCDA reduced species can concomitantly be formed and co-precipitated with bayerite. This process occurs dynamically, in which aluminum has to be initially stripped from the outer oxide layer, then the NTCDA enters the crevices (pits of the alkaline corrosion) or adsorbs onto aluminum surface and forms the radical anions, which are subsequently reticulated together with the precipitation of the bayerite crystallites from the aluminate solution; once generated they are kept intact with respect to hydrolysis reaction and reaction with oxygen.

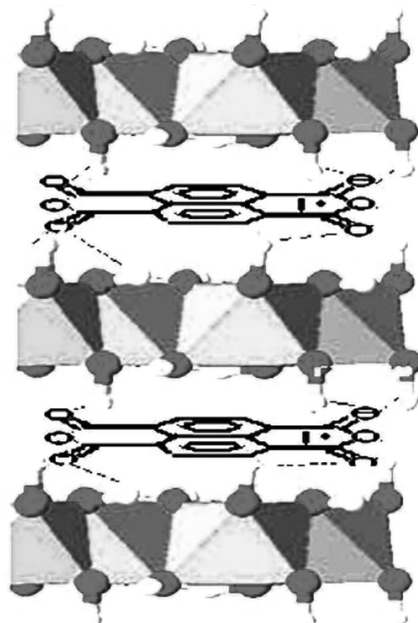


**Figure 8.** Inclusion of the NTCDA<sup>1-</sup> into layered double hydroxide of the bayerite structure.

## 4. Conclusions

The reaction between NTCDA and aluminum presents a clear dependence on the solvent composition in hydro-alcoholic solutions. In EtOH-H<sub>2</sub>O (1:3, v:v) mixtures the formation of NTCDA electron-adducts is accomplished, in addition to a hydrolysis side reaction. The amount of base also affects the reductive process, since more base leads to the dianion and lower concentrations favor the radical monoanion formation. In EtOH-H<sub>2</sub>O (3:1, v:v) there was the precipitation of a powder identified as bayerite [ $\alpha$ -Al(OH)<sub>3</sub>] that has paramagnetic organic species ( $g = 2,006$ ) entrapped which are stable to air exposure for more than one year and also thermally stable up to 200 °C. The UV-VIS, ESR and IR spectra point to NTCDA radical species within the bayerite inorganic matrix. These species are possibly trapped between the sheets of the bayerite structure by hydrogen bonds between the dianhydride's carbonyls and hydroxides of the bayerite sheets. Two main points can be pointed out concerning the work here described. First, it is a selective experimental methodology for aluminum trihydroxide bayerite formation. Second, it may be an alternative to the preparation of hybrid organic-inorganic materials based on bayerite composites.

## Acknowledgments

The support of the Brazilian grant agencies FAPESP, Proc. 04/15069-7, CNPQ and CAPES are acknowledged. We wish to express our gratitude to Dr. Marcelo Porto Bemquerer and Shirley Schreier for the interesting and helpful discussions.

## References

- Thalacker C, Röger C and Würthner F. Synthesis and Optical and redox properties of core-substituted naphthalene diimide dyes. *Journal of Organic Chemistry*. 2006; 71(21):8098-8105.
- Erten S, Posokhov Y, Alp S and İçli S. The study of the solubility of naphthalene diimides with various bulky flanking substituents in different solvents by UV-vis spectroscopy. *Dyes and Pigments*. 2005; 64(2):171-178.
- Abraham B, McMasters S, Mullan MA and Kelly LA. Self-assembly of naphthalene diimides into cylindrical microstructures. *Journal of American Chemical Society*. 2004; 126(13):4293-4300.
- Alivisatos AP, Barbara PF, Castleman AW, Chang J, Dixon DA, Klein ML et al. From molecules to materials: Current trends and future directions. *Advanced Materials*. 1998; 10(16):1297-1336.
- Facchetti A. Semiconductors for organic transistors. *Materials Today*. 2007; 10(3):28-37.
- Amy F, Chan C and Kahn A. Polarization at the gold-pentacene interface. *Organic Electronics*. 2005; 6(2):85-91.
- Nakayama K, Niguma Y, Matsui Y and Yokoyama M. Electronic interactions in codeposited films of naphthalene tetracarboxylic derivatives and metals. *Journal of Applied Physics*. 2003; 94(5):3216-3221.
- Fink R, Gador D, Stahl U, Zou Y and Umbach E. Substrate-dependent lateral order in naphthalene-tetracarboxylic-dianhydride monolayers. *Physical Review B*. 1999; 60(4):2818-2826.
- Yamaguchi H, Kitano K, Toyoda K and Baumann H. Magnetic circular dichroism spectra of naphthalic anhydride and 1,4,5,8-naphthalenetetracarboxylic and 1,4,5,8-dianhydride. *Spectrochimica Acta A*. 1982; 38(2):261-263.
- Adachi M, Murata Y and Nakamura S. Spectral similarity and difference of naphthalenetetracarboxylic dianhydride, perylenetetracarboxylic dianhydride, and their derivatives. *Journal of Physical Chemistry*. 1995; 99(39):14240-14246.
- Barros TC, Cuccovia IM, Farah JPS, Masini JC, Chaimovich H and Politi MJ. Mechanism of 1,4,5,8-naphthalene tetracarboxylic acid dianhydride hydrolysis and formation in aqueous solution. *Organic and Biomolecular Chemistry*. 2006; 4(1):71-82.
- De Luca C, Giomini C and Rampazzo L. The multi-step reversible reduction of 1,4,5,8-naphthalene tetracarboxylic acid dianhydride: an electrochemical study. *Journal of Electroanalytical Chemistry*. 1990; 280(1):145-157.
- Nelsen SF. Heterocyclic Radical Ions II. Naphthalic and 1,4,5,8-Naphthalene Tetracarboxylic Acid Derivatives. *Journal of American Chemical Society*. 1967; 89:5925-5931.
- Heywang G, Born L, Fitzky H-G, Hassel T, Hocker J, Müller H-K et al. Radical anion salts of naphthalenetetracarboxylic acid derivatives - a novel class of electrically conducting compounds. *Angewandte Chemie International Edition English*. 1989; 28(4):483-485.
- Rodrigues MA, Bemquerer MP, Mohallem NDS and Politi MJ. Xerogel from N,N'-Bis(2-phosphonoethyl)1,4,5,8-naphthalenediimide: a nanohybrid material displaying efficient tryptophan photooxidation. *Langmuir*. 2006; 22(21):8939-8944.
- Demichelis R, Civalleri B, Noel Y, Meyer A and Dovesi R. *Ab initio* quantum mechanical study of akdalaite (5Al<sub>2</sub>O<sub>3</sub> · H<sub>2</sub>O): structure and vibrational spectrum. *Chemical Physics Letters*. 2008; 465:220-225.
- Gale JD, Rohl AL, Milman V and Warren MC. An *Ab initio* study of the structure and properties of the polymorphs of aluminium hydroxide. *Journal of Physical Chemistry B*. 2001; 105(42):10236-10242.
- Coelho ACV, Santos HS, Kiyohara PK, Marcos KNP and Santos PS. Surface area, crystal morphology and characterization of transition alumina powders from a new gibbsite precursor. *Materials Research*. 2007; 10(2):183-189.
- Oliveira IR and Pandolfelli VC. Refractory castables prepared with hydratable alumina: the dispersant effect. *Cerâmica*. 2009; 55(333):33-39.
- Zhang B, Li J, Chen Q and Chen G. Precipitation of Al(OH)<sub>3</sub> crystals from supersaturated sodium aluminate solution irradiated with ultrasonic sound. *Minerals Engineering*. 2009; 22(9-10):853-858.
- Antunes MLP, Santos HS and Santos PS. Characterization of the aluminum hydroxide microcrystals formed in some alcohol-water solutions. *Materials Chemistry and Physics*. 2002; 76:243-249.
- Harris DR, Keir RI, Prestidge CA and Thomas JC. A dynamic light scattering investigation of nucleation and growth in supersaturated alkaline sodium aluminate solutions (synthetic Bayer liquors). *Colloids And Surfaces A: Physicochemical and Engineering Aspects*. 1999; 154(3):343-352.
- Prestidge CA and Ametov I. Cation effects during aggregation and agglomeration of gibbsite particles under synthetic bayer crystallisation conditions. *Journal of Crystal Growth*. 2000; 209(4):924-933.
- Sipos P, Hefter G and May PM. A hydrogen electrode study of concentrated alkaline aluminate solutions. *Australian Journal of Chemistry*. 1998; 51(6):445-453.
- Britto S, Thomas GS, Kamath PV and Kannan S. Polymorphism and structural disorder in the carbonate containing layered double hydroxide of Li with Al. *Journal of Physical Chemistry C*. 2008; 112(25):9510-9515.
- Lei L, Zhang W, Hu M and Zheng H. Alkaline hydrolysis of dimethyl terephthalate in the presence of [LiAl<sub>2</sub>(OH)<sub>6</sub>]Cl·2H<sub>2</sub>O. *Journal of Solid State Chemistry*. 2006; 179(11):3562-3567.
- Fogg AM, Dunn JS, Shyu S-G, Cary DR and O'Hare D. New separation science using shape-selective ion exchange intercalation chemistry. *Advanced Materials*. 1999; 11(17):1466-1469.
- Lefèvre G, Pichot V and Fédoroff M. Controlling particle morphology during growth of bayerite in aluminate solutions. *Chemistry of Materials*. 2003; 15(13):2584-2592.
- Hiemstra T, Young H and Van Riemsdijk WH. Effect of different crystal faces on experimental interaction force and aggregation of hematite. *Langmuir*. 1999; 15(23):8045-8051.
- Van Straten HA, Schoonen MAA and De Bruyn PL. precipitation from supersaturated aluminate solutions. *Journal of Colloids and Interface Science*. 1985; 103(2):493-507.
- Phambu N, Humbert B and Burneau A. Relation between the infrared spectra and the lateral specific surface areas of gibbsite samples. *Langmuir*. 2000; 16(15):6200-6207.

32. Tanaka H and Kuroboshi M. Aluminium as an electron pool for organic synthesis. Multi-metal redox-promoted reactions. *Current Organic Chemistry*. 2004; 8:1027-1056.
33. Sarmah P and Barva NC. A facile reduction procedure for nitroarenes with  $\text{NiCl}_2$ -THF system. *Tetrahedron Letters*. 1990;31(28):4065-4066.
34. Khurana JM and Singh S. Reductive coupling of nitroarenes to hydrazoarenes with aluminium and potassium hydroxide in methanol. *Journal of the Chemical Society, Perkin. Transaction. I*. 1999; 13:1893-1895.
35. Nagaraja D and Pasha MA. Reduction of aryl nitro compounds with aluminum/ $\text{NH}_4\text{Cl}$ : effect of ultrasound on the rate of the reaction. *Tetrahedron Letters*. 1999; 40(44):7855-7856.
36. Huffman JW. *Comprehensive organic synthesis*. Oxford: Pergamon; v. 8, 1991.
37. Becker H. *Organikum*. 2<sup>nd</sup> ed. Lisboa: Calouste Gulbenkian; 1997.
38. Wudl F and Bryce MR. Apparatus for two-probe conductivity measurements on compressed powders. *Journal of Chemical Education*. 1990; 67(8):717-718.
39. Rodrigues MA, Bemquerer MP, Politi MJ and Baptista MS. Electron transfer, charge stabilization and charge recombination in naphthalenediimide-tryptophan immobilized on silica particles. *Journal of Photochemistry and Photobiology A: Chemistry*. 2006; 180(1-2):218-221.
40. Andric G, Boas JF, Bond AM, Fallon GD, Ghiggino KP, Hogan CF et al. Spectroscopy of Naphthalene Diimides and their anion radicals. *Australian Journal of Chemistry*. 2004; 57(10):1011-1019.
41. Deltombe E, Vanleughenaghe C and Pourbaix M. *Atlas of electrochemical equilibria in aqueous solutions*. New York: Pergamon; 1966.
42. Adhikari S, Lee J and Hebert K. Formation of aluminum hydride during alkaline dissolution of aluminum. *Journal of Electrochemical Society*. 2008; 155(1):16-21.
43. Zhang Y, Zheng S, Du H, Xu H, Wang S and Zhang Y. Improved precipitation of gibbsite from sodium aluminate solution by adding methanol. *Hydrometallurgy*. 2009; 98(1-2):38-44.
44. Jones DA. *Thermodynamic and electrode potential. Principles and prevention of corrosion*. 2<sup>nd</sup> ed. New Jersey: Prentice Hall; 1996.
45. Uhlig HH and Revie RW. *Corrosion and corrosion control*. 3<sup>rd</sup> ed. New York: Wiley-Interscience; 1985.
46. Sidrak YL. Dynamic simulation approach to digester ratio control in alumina production. *Industrial & Engineering Chemical Research*. 1998; 37(4):1404-1409.
47. Orvig C. *The aqueous coordination chemistry of aluminum*. New York: VCH; 1993.
48. Adhikari S, Lee J and Hebert KR. Formation of aluminum hydride during alkaline dissolution of aluminum. *Journal of Electrochemical Society*. 2008; 155(1):C16-C21.
49. Landsberg B, McDonald B and Watt F. Absence of aluminium in neuritic plaque cores in Alzheimer's disease. *Nature*. 1992; 360(6399):65-68.
50. Swaddle TW, Salerno J and Tregloan PA. Aqueous aluminates, silicates, and aluminosilicates. *Chemical Society Review*. 1994; 23:319-325.
51. Sipos P. The structure of Al(III) in strongly alkaline aluminate solutions - A review. *Journal of Molecular Liquids*. 2009; 146(1-2):1-14.
52. Balan E, Blanchard M, Hochepeid J-F and Lazerri M. Surface modes in the infrared spectrum of hydrous minerals: the OH stretching modes of bayerite. *Physics and Chemistry of Minerals*. 2008; 35(5):279-285.
53. Tachikawa H, Kawabata H, Miyamoto R, Nakayama K and Yokoyama M. Experimental and theoretical studies on the organic-inorganic hybrid compound: aluminum-NTCDA co-deposited film. *Journal of Physical Chemistry B*. 2005; 109(8):3139-3145.
54. Braddock WJ, Leman JT, Farrar CT, Larsen SC, Singel DJ and Barron AR. Radical anion complexes of tris-(1,3-diphenyltriazenido)aluminum. *Journal of American Chemical Society*. 1995; 117:1736-1745.
55. Dunn B and Farrington GC. Fast Divalent Ion Conduction in  $\text{Ba}^{++}$ ,  $\text{Cd}^{++}$ , and  $\text{Sr}^{++}$  Beta'-Alumina. *Materials Research Bulletin*. 1980; 15:1773-1777.
56. Tomasulo M, Naistat DM, White AJP, Williams DJ and Raymo FM. Self-assembly of naphthalene diimides into cylindrical microstructures. *Tetrahedron Letters*. 2005; 46(34):5695-5698.
57. Ofir Y, Zelichenok A and Yitzchaik S. 1,4,5,8-naphthalene-tetracarboxylic diimide derivatives as model compounds for molecular layer epitaxy. *Journal of Materials Chemistry*. 2006; 16:2142-2149.
58. Goynes KW, Chorover J, Kubicki JD, Zimmerman AR and Brantley SL. Sorption of the antibiotic ofloxacin to mesoporous and nonporous alumina and silica. *Journal of Colloids and Interface Science*. 2005; 283(1):160-170.
59. Rat'ko AI, Kuznetsova TF, Romanenkov VE and Klevchenya DI. kinetics of bayerite microstructure formation from powdered aluminum. *Colloid Journal*. 2008; 70(2):210-214.
60. Rat'ko AI, Romanenkov VE, Bolotnikova EV and Krupen'kina ZhV. Hydrothermal Synthesis of porous  $\text{Al}_2\text{O}_3/\text{Al}$  metal ceramics: IV. Synthesis of composite porous ceramics in the presence of microporous and mesoporous adsorbents. *Kinetics and Catalysis*. 2004; 45(2):279-287.